Fall 12-20-2022

Manganese Chloride Effects Chondrogenesis of ATDC5 Cells

Isabella Somera
isabella.somera@student.shu.edu

MANGANESE CHLORIDE EFFECTS CHONDROGENESIS OF ATDC5 CELLS

By

Isabella K. Somera

Submitted in partial fulfillment of the requirements for the degree Master of Science in Biology from the Department of Biological Sciences of Seton Hall University December, 2022.

SETON HALL UNIVERSITY
College of Arts and Sciences
Department of Biological Sciences

APPROVAL FOR SUCCESSFUL DEFENSE

Isabella K. Somera has successfully defended and made the required modifications to the text of her master's thesis for **M.S. Biology** during this **Fall Semester 2022**.

THESIS COMMITTEE

(Please sign and date beside your name)

_____

MENTOR
Dr. Jessica Cottrell

_____

COMMITTEE MEMBER
Dr. Daniel Brian Nichols

_____

COMMITTEE MEMBER
Dr. Constantine Bitsaktsis

_____

DIRECTOR OF GRADUATE STUDIES
Dr. Constantine Bitsaktsis

_____

CHAIRPERSON, DEPARTMENT OF BIOLOGICAL SCIENCES
Dr. Jessica Cottrell

Acknowledgements:

First and foremost, I would like to thank God for the opportunity to pursue my M.S. degree and for allowing me to encounter all my peers, professors, and friends at Seton Hall University. I would especially like to thank my committee members, Dr. Daniel Brian Nichols and Dr. Constantine Bitsaktsis, for their time and enthusiasm to join me in this milestone.

Thank you to my mom and dad for providing me with the means to always reach my goals. Thank you also to Michael Rangel for reminding me to dream big and for sharing a big dream together with me. I cannot imagine pursuing this endeavor without you all in my life.

I would like to thank my fellow grad students, Amber Chaudhary, Matthew Gregory, Lea Marjana, Brian Reiss, Nicolas Ebner, Helena Schmittberger, and Alexandra Bambrick for their ceaseless support, unmatched wit, and priceless friendships. It has been exceptional to navigate grad school with you all.

Thank you also to the undergrads, Nikki, Priyanka, Ricky, Matt, Susan, and Alyssa, for their efforts and talents in assisting me with my thesis experiments. It has been a joy not only teaching you all, but also learning, from you in lab. I would like to also extend my appreciation to the other members of the Cottrell Lab.

Most of all, thank you to my mentor, Dr. Jessica Cottrell, for imparting with me some of the greatest lessons, not just at the lab bench, but in life as well. I cannot thank you enough for your patience, lightheartedness, and sense of grounding you impart to everyone you meet.

Table of Contents:

Abstract

Manganese is an essential trace element found in humans, which aids in several processes including brain and nerve function, glucose metabolism, calcium absorption, and bone formation and homeostasis. Specifically, bone homeostasis utilizes osteoblasts and osteoclasts, cells which function to build and reabsorb bone respectively, as well as chondrocytes, cells which aid in endochondral ossification. Chondrocytes deposit extracellular matrix components, such as aggrecan, collagen, and proteoglycans, that provide the necessary scaffold for osteoblasts to synthesize and mineralize bone. Activation of the rapamycin (mTOR) pathway influences the regulation of several cellular processes, such as skeletal development and bone homeostasis. In this study, it was hypothesized that Manganese Chloride ($MnCl_2$) treatments would activate the RHEB/mTOR pathway in the murine ATDC5 cell line to enhance chondrocyte maturation and protection against degradation. To test this hypothesis, the effects of $MnCl_2$ treated ATDC5 cells were measured through cellular proliferation, alkaline phosphatase activity, calcium deposition, proteoglycan concentrations, and gene expression at timepoints. Our results found that $MnCl_2$ dose dependently decreased chondrocyte proliferation and proteoglycan deposition, while increasing alkaline phosphatase activity and calcium deposition.

Keywords: Manganese chloride, chondrogenesis, chondrocyte, hypertrophic cartilage, endochondral ossification, osteoarthritis, mTOR pathway, RHEB, alkaline phosphatase, proteoglycan

Introduction

Manganese Chloride

Manganese is an essential trace element found in the human diet. This element aids in carbohydrate, protein, and cholesterol metabolism (1). Not only does it support normal brain and nerve function, but manganese also aids in the formation of connective tissues, calcium absorption, and bone matrices (1, 2). Studies have shown that manganese functions as an antioxidant factor and enzyme cofactor for enzyme superoxide dismutase (SOD), which allows the body to fight against harmful free radicals (1). Manganese also been shown to aid Vitamin K in blood clotting and wound healing (3).

Cartilage Formation / Chondrogenesis

Chondrocytes are responsible for synthesizing extracellular matrix (ECM) components, collagen, specifically Collagen Type II (Col2a1), and proteoglycans, all which provide the necessary scaffold for bone synthesis (4). Without healthy chondrocytes secreting these components, matrix degradation occurs, initiating and progressing into diseases such as Osteoarthritis (OA) down the line (4). Chondrogenesis begins with the condensation of mesenchymal cells (MSC), differentiation into chondroprogenitors, maturation into chondroblasts and chondrocytes, and finally terminal differentiation into hypertrophic chondrocytes. During this process, chondrocytes express Collagens I-X as they mature (**Figure 1)** (4). The presence of important transcription factors, such as SRY-box 9 protein (SOX9) and Runt-related transcription factor 2 (RUNX2), allow for smooth chondrocyte development, and are responsible for MSC differentiation and hypertrophic chondrocyte stimulation, respectively (5). Bone morphogenic proteins (BMPs) regulate the expression of both SOX9 and RUNX2 (5).

Extracellular matrix proteins, such as Col1 and Col2a1, are secreted between MSC condensation and chondroprogenitor differentiation, and are responsible for tissue strengthening and matrix stabilization (6). Col2a1 comprises 90% of ECM collagen, creating a fibrous network with proteoglycan-like aggrecans (6). Chondrocytes deposit cartilage at the ends of bones, undergoing a cycle of proliferation, hypertrophy, and apoptosis to allow endochondral ossification, the process wherein hypertrophic cartilage is reabsorbed and replaced by bone, to occur (7).

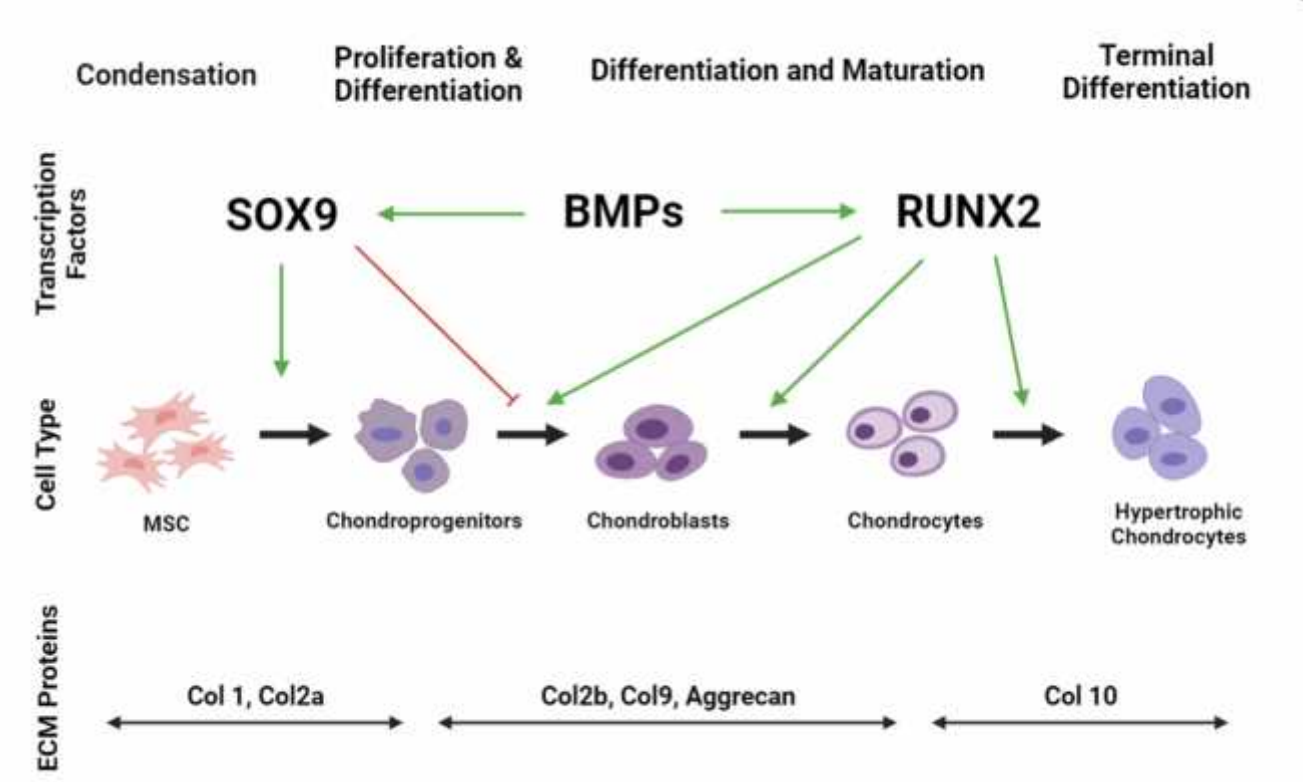

Note: Figure made by Isabella K. Somera using BioRender.com

Figure 1: Stages of Chondrogenesis

Chondrogenesis begins with MSC condensation, which is controlled by transcription factor, SOX9. During this stage, Col2a1 is expressed in the ECM. MSCs proliferate and differentiate into chondroprogenitors and mature into hypertrophic chondrocytes, which is controlled by RUNX2. Hypertrophic chondrocytes will then begin endochondral ossification. BMPs control both SOX9 and RUNX2 expression.

Manganese Chloride and Chondrogenesis

Although the pathway of activation in the body is still unclear, manganese's effect on chondrogenesis can be observed through the delay of articular cartilage regeneration and cartilage repair (1). Additionally, manganese aids in the synthesis of glycosaminoglycans, proteoglycans, Col2a1, regulation of cartilage matrix metabolism, scavenging oxygen free radical and antioxidants, reducing oxidative stress, and protecting the ECM (1). The deficiency of manganese disrupts glycosaminoglycan biosynthesis and chondrogenesis, leading to cartilage dysplasia and lack of endochondral bone formations (1, 8). According to Cue-Yue Wang, who studied the deficiencies of this trace element in the cartilaginous dystrophy disease, avian tibial dyschondroplasia (TD), saw that the lack of manganese disrupts normal chondrocyte growth in the tibial growth plate and lowers protein expression of Col2a1 and Collagen Type X (9). Additionally, Wang performed histological staining which illustrated atypical chondrocyte morphologies and arrangements, that were associated with inhibited endochondral ossification (9). In another study, manganese deficiency on chondrocyte development of the tibial growth plate was conducted on Arbor Acres chicks. In this study, manganese deficient chicks showed bone perosis, resulting in enlarged distal tibias and distorted proximal tibias (10). Histopathological observations saw reduced proliferation zones of manganese deficient growth plates, as reflected in the abnormal tibial growth (10). Jian Wang also reported increased apoptosis of hypertrophic chondrocytes due to manganese deficiency (10).

Osteoarthritis

Osteoarthritis (OA) is a chronic degenerative joint disease, which specifically deteriorates the structure of articular cartilage found at the ends of bones over time. Over 32.5 million US adults are affected with OA, and experience symptoms of pain, stiffness, and immobility due to aging, mechanical stresses, and localized inflammation (11,12). There is no specific cure for this disease, but various treatments to relieve patient including nonsteroidal anti-inflammatory drugs (NSAIDS), cortisone or lubrication injections, and surgical measures, such as knee osteotomies (11, 13). Unfortunately, these nonsurgical and reconstructive surgical therapies do not effectively resolve OA as cartilage has low levels of perfusion, or vascularity, which restrict its ability to regenerate and self-repair (14, 15). Current gene and regenerative therapies have sought to solve this issue. For example, autologous chondrocyte implantation (ACI) is a current medical treatment which aims to rebuild articular tissues (12). Although ACI shows promise for cartilage tissue regeneration, ACI requires specific amounts of clinical-grade chondrocytes for successful therapy (12). *In vitro* cultures are necessary in the transplantation process, but also present challenges regarding the replication of physiological human chondrocyte activity (12). *In vitro* chondrocytes cultures face challenges of senescence, dedifferentiation, and oxidative stresses with exposure to reactive oxygen species with every cell passage (12). Senescent chondrocytes enter a state of irreversible growth arrest and dedifferentiate with phenotypic changes from polygonal to a fibroblastic morphology (12). Additionally, less aggrecan and Col2a1 are expressed, while increased hypertrophic markers, such as Col10a1, are shown (12). Reactive oxygen species (ROS) and cell senescence inhibit proteoglycan synthesis and growth of the ECM, and overtime, can adversely affect cartilage (4,7).

Osteoarthritis & RHEB

Ras homolog enriched in brain (RHEB) is a guanosine triphosphate (GTPase), which belongs to the Ras superfamily, and aids in the regulation of cell growth, proliferation, and differentiation (16). RHEB targeting has been able to increase chondrogenic markers in healthy chondrocytes as well as degenerated OA chondrocytes (16). RHEB is essential in the activation of mammalian target of rapamycin (mTOR), a serine/threonine kinase responsible for protein synthesis, growth, and autophagy **(Figure 2)** (16,17). mTOR has two subunits: mTORC1 and mTORC2 (16). mTORC1 monitors signals of growth factors such as Insulin/Insulin Growth Factor-1 (IGF-1), oxygen and energy levels for cell growth and metabolism (16). RHEB can directly bind to mTORC1 and stimulate this activity (16). Conversely, mTORC2 controls proliferation and survival, but is activated through mechanical stress and ribosomes *in vitro* (16). mTORC1 has been said to aid in the regulation of cartilage development, primarily through its disruption, which impaired chondrogenesis (16). In terms of OA, mTOR appears to be overexpressed in human, rodent, and canine experiments (17). The upregulation of mTOR caused a direct downstream modulation of autophagy in articular cartilage homeostasis (17).

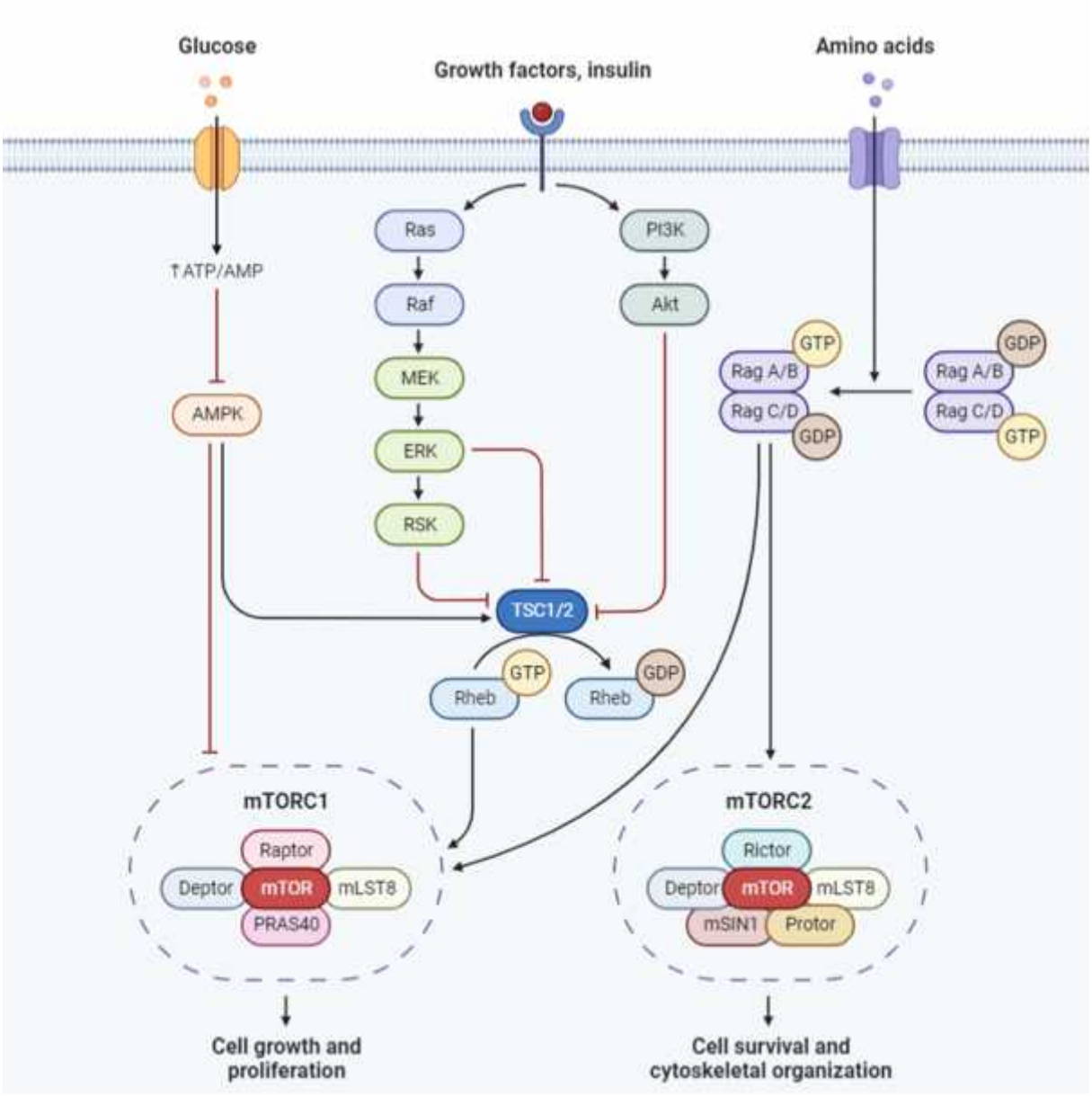

Note: Figure made using BioRender.com

Figure 2: mTOR Signaling Pathway

The targeting of RHEB has been shown to upregulate expression of chondrocyte markers in both healthy and OA chondrocytes. RHEB is responsible for activating mTOR subunit, mTORC1, which leads to cell growth and proliferation.

Manganese Chloride and RHEB

Little is known regarding manganese and RHEB, but manganese appears to activate and regulate TORC1 in yeast (mTORC1 in mammals) for manganese homeostasis (17). Interestingly, manganese could activate the Protein Kinase B (AKT) / Tuberous Sclerosis Complex 2 (TSC2) pathway, leading to RHEB and mTOR activation (18). Additionally, the activity of Kisspeptin-1 (KISS1) was explored due to activation of the AKT/RHEB/mTOR pathway (18). Therefore, in this present study, the interactions between manganese chloride, RHEB, and mTOR will be explored in hopes to find a potential target for gene therapy for osteoarthritis. We hypothesized that manganese chloride will have a positive effect on chondrocyte viability, alkaline phosphatase (ALP) activity, calcium deposition, and proteoglycan deposition.

Methodology:

Cell Culture

ATDC5 murine chondrocyte cells were gifted from the O'Connor Lab (Rutgers New Jersey Medical School, Newark, NJ), and were cultured in growth medium containing Delbecco's Modified Eagle's Medium (DMEM F12 50/50) (Corning, Corning NY), supplemented with 5% fetal bovine serum (FBS) (Atlanta Biologics), 1% Penicillin/Streptomycin (Corning, Corning NY), 1% Glutamate (Corning, Corning NY), 1% Transferrin (Invitrogen, Waltham MA) and 1% Sodium Selenite (Sigma-Aldrich, Burlington MA). Cells were stored in an incubator of 5% CO_2 at 37 , and were passaged up to 8 times. Seedings of 100,000 cells per well (30% density) were completed in 12-well plates. Chondrogenesis was maintained with frequent media exchanges with differentiation medium. The differentiation medium consisted of a positive control of 10µg/mL of insulin (Sigma-Aldrich, Burlington MA), negative control of basal media, and increasing concentrations of $MnCl_2$ (Sigma-Aldrich, Burlington MA) at low dose (0.3µM), medium dose (3µM), and high dose (30µM). Media exchanges occurred every 2-3 days, and cell media was collected post-treatment on Days 1, 3, 7, 10, 14, 17, and 21.

MTT Assay (Cellular Viability and Proliferation)

To evaluate cellular proliferation induced by $MnCl_2$, an MTT Assay Kit (Abcam, Cambridge UK) was completed. First, ATDC5 cells were plated at a density of 20,000 cells in a 96-well plate and were left to incubate at 37 . Treatments of insulin and increasing doses of $MnCl_2$ were added 24 hours after plating. MTT solution was added after 24 hours of treatment left to incubate at 37 for 3 hours. Following incubation, DMSO was added to each well and

again was left to incubate for 2-6 hours. Absorbances of the plates were read in triplicate at 570nm. After the data was normalized, the Percent Viability was calculated using the equation:

$$Percent\ Viability = \frac{Normalized\ Treatment\ Value}{Mean\ of\ Negative\ Control} \times 100\ .$$

Alkaline Phosphatase (ALP) Assay

To study ALP activity, an indicator of the presence of osteoblasts and formation of new bones, an ALP Assay (Abcam, Cambridge UK) was performed. The media collected from Days 1, 3, 7, 10, and 14 were used to quantify ALP activity. Standards, samples diluted with Assay Buffer, and sample background controls were added in triplicate to a 96-well plate. After, 5 mM *p*NPP solution was added to the sample and background control wells with the ALP enzyme added to the standard wells. Plates were left to incubate at 25°C for 60 minutes on a shaker and protected from light. Absorbance was read at 405nm. A standard curve was used to generate concentrations of ALP.

Alizarin Red Staining (Calcium Deposition)

To assess calcium deposition within the cell cultures, an Alizarin Red Stain (ARS), was performed. This anthraquinone dye can be extracted from the stained monolayer of cells and can be used in order to quantify calcification. At day 14, the cells were gently washed with 1x Phosphate Buffer Saline (PBS) (ThermoFisher, Waltham MA) and fixed in 4% formaldehyde for 15 minutes at room temperature. After the fixative was aspirated, the cells were washed 3 times with diH_20 and stained with 1mL of 40 mM ARS per well. The plates were then incubated at room temperature and left on plate shaker for 25 minutes. Then, the dye was removed and washed 5 times with diH_20 and imaged using the Accu-Scope Microscope (ACCU-SCOPE Inc.,

Commack NY) Then, 10% acetic acid was added to each well and incubated at room temperature for 30 minutes with shaking. The cells were then collected with a cell scraper and transferred in the 10% acetic acid to a microcentrifuge tube. After, the tubes were vortexed, heated at 85 for 10 minutes, and placed on ice for 5 minutes. The slurry was then centrifuged at 20,000g for 15 minutes and the supernatant was transferred and combined with 10% ammonium hydroxide (WVR, Randor PA) to neutralize the acid in a new tube. Samples were aliquoted in triplicate into a flat-bottom 96-well plate and measured at an absorbance of 405nm using the VarioSkan Plate Reader (ThermoFisher, Waltham MA). An ARS standard curve was generated to calculate the concentrations of calcium deposition of the samples.

Glacial Blue Assay (Proteoglycan Deposition)

To measure the levels of proteoglycan, an essential chondrocyte cell marker, the Alcian Blue Staining was performed. Cells were fixed with 100% cold methanol for 5 minutes and then 0.1% Alcian Blue in 0.1M HCl was added overnight. After washing the cells three times with 1x PBS, the alcian blue was extracted overnight with 6M Guanidine-HCl on an orbital shaker at 4 . The samples were then read at an absorbance of 595nm.

RNA Isolation (Zymo Research)

Following treatment, cells were harvested on Days 1, 3, and 7. Wells were aspirated of any media and washed with 1x PBS (ThermoFisher, Waltham MA). Using a cell scraper, the cells were extracted and transferred to an autoclaved microcentrifuge tube for centrifugation. To separate pure RNA, the Direct-zol RNA MicroPrep Kit (Zymo Research, Irving CA) was used. All steps were performed at room temperature with samples kept on ice and centrifuged at

10,000 x g for 30 seconds, unless specified. The PBS supernatant was aspirated, and the pellet was resuspended in 350µL of TRI Reagent buffer (Zymo Research, Irving CA). An equal volume of 350µL of 95-100% ethanol was added to the lysed sample (Zymo Research, Irving CA). The mixture was transferred into a Zymo-Spin IC Column placed in a collection tube and centrifuged. The spin column was placed into a new collection tube and the flow-through was discarded. Next, 400µL of Direct-zol RNA Pre-Wash (Zymo Research, Irving CA) was added to the column and centrifuged. The flow through was discarded and the above step was repeated. Then, 700µL of RNA Wash Buffer (Zymo Research, Irving CA) was added to the column and centrifuged for 1 minute to ensure complete removal of the wash buffer. The column was then transferred carefully into an RNase-free tube. RNA was then eluted into 15µL of autoclaved Dnase/Rnase free water and added directly onto the column matrix and centrifuged. The concentrations and purity of RNA were measured using the BioDrop Duo (Biodrop, Cambridge UK). The samples were stored in the -80 to prevent denaturation.

Reverse Transcriptase

To synthesize cDNA from the RNA isolates, 100ng of each RNA sample was diluted with Dnase/Rnase free water for a total of 12µL and prepared as the reaction tubes. Depending on the number of samples, 4µL of Master Mix I made with 2µL of 5mM dNTPs and 2µL of oligo dTs were added to the sample reaction tubes. The reaction tubes were then vortexed, centrifuged, secured with fasteners, and placed in a 65 MyBlock hot bath (Benchmark Scientific Inc., Sayreville NJ) for 3 minutes, and returned to ice. Next, 3µL of Master Mix II made with 2µL of 10x MM-LVRT Buffer (Biolabs, Boston MA) and 1µL of Rnase Inhibitor (Biolabs, Boston MA) were added to the reaction tubes. The enzyme was added separately with

1µL of MM-LVRT (Lucigen, Middleton WI) to the reaction tubes, and then vortexed and centrifuged. The reaction tubes were then placed in a 42 Isotemp water bath (ThermoFisher Scientific, Hampton NH) for 1 hour. After the incubation, the reaction tubes were spun down quickly, secured with fasteners, and placed in a 95 hot bath for 10 minutes. The reaction tubes were then allowed to cool to room temperature before using the Biodrop (Biodrop, Cambridge UK) to quantify the cDNA.

Polymerase Chain Reaction (PCR)

To confirm the presence of cDNA, PCR was ran using GAPDH. First, a 10µM Working Primer Solution of GAPDH (Invitrogen, Waltham MA) was made from 10µL Forward and 10µL Reverse primer stocks of 100µM and diluted with 80µL of Dnase/Rnase free water. Then, Master Mix I was made with 2.5µL 10X Standard Taq Reaction Buffer (Biolabs, Boston MA) 1µL of 10µM dNTPs, 1µL of 10µM GAPDH Working Primer Solution, 17.875µL of Dnase/Rnase free water, and 0.125µL of Taq DNA Polymerase Enzyme (Biolabs, Boston MA). Each amount was multiplied by the number samples, and 22.5µL of Master Mix and 2.5µL of cDNA was added to PCR tubes. The PCR tubes were vortexed and spun down before loading into the PCR T100 Thermal Cycler (BioRad, Hercules CA). The PCR program for Taq called for Initial Denaturation of 95 for 30 seconds, 30 cycles of 95 for 15-30 seconds, 60 for 15-60 seconds, 68 for 1 minute/kb, Final Extension for 68 for 5 minutes, and a hold for 4-10 . The PCR samples were then transferred to the -80 for storage.

Table 1: PCR Thermocycler Program

	Temperature ( )	Time	Number of Cycles
Initial Denaturation	95	30 sec	
Denaturation	95	30 sec	30
Annealing	60	30 sec	30
Extension	68	1 min	30
Final Extension	68	5 min	
Hold	4	∞	

DNA Gel Electrophoresis

To verify the success of the RT-preps, a 2% gel was made with 0.5g agarose and 25mL of Tris-Acetate-EDTA (TAE) Buffer 10X Liquid Concentrate (Hoefer Inc, Hollisten MA). Agarose, electrophoresis grade (MP Biomedicals, Santa Ana CA) and TAE buffer were combined in an Erlenmeyer flask, heated for periods of 10-30 seconds in the microwaved, and swirled until the solution was clear and homogeneous. Once the Horizon 58 Gel Box (Life Technologies, Carlsbad CA) was properly set up, the agarose solution was poured into the gel case with an 8-well comb and left to cool for 20-25 minutes. Once the gel was fully solidified, the comb was carefully removed, and the gel was submerged in 1x TAE buffer. The first well was loaded with 4µL of DNA Marker 100bp Ladder (Denville Scientific, South Painfield NJ) followed by 10µL of sample and 5µL of 5x DNA loading dye, which was combined over a square of parafilm. The EC300XL Electrophoresis Power Supply (ThermoScientific, Waltham MA) ran at conditions of 90V at 120mA for 1 hour. The gel was then carefully transferred to a small box and submerged with DI water. The gel was left to shake for 10 minutes with 2-4µL of Ethidium Bromide Solution (G BioSciences, St. Louis MO). The gels were then imaged on the FluorChem machine (ProteinSimple, Santa Clara CA) on a clear plate.

Quantitative Polymerase Chain Reaction (qPCR)

To amplify cDNA for the gene expression, qPCR was completed. First, cDNA samples were diluted 1:20 (5µL:95µL Rnase/Dnase free water) and the respective 5µM Working Primer Solutions were made. After, a Master Mix of 10µL Zymo*Taq* qPCR PreMix (Irvine, CA), 3µL 5µM Working Primer Mix, 6.5µL Rnase/Dnase free water, and 2.5µL of cDNA sample were added to a 384-well plate. Volumes of the Master Mix were determined by the number of samples needed for the experiment.

Table 2: qPCR Thermal and Melt Curve Programs

	Temperature ( )	**Time**	**Number of Cycles**
Initial Denaturation	95	10 min	40
Denaturation	95	30 sec	40
Annealing	60	30 sec	40
Extension	72	15-30 sec	40
Final Extension	72	7 min	
Hold	4	> 4 min	

Table 3: Primer Sequences

Oligo Name	**Sequence**
B-Actin_R	GACAGGATGCAGAAGGAGATTACTG
B-Actin_F	CCACCGATCCACACAGAGTACTT
RHEB_F	AAGTCCCGGAAGATCGCCA
RHEB_R	GGTTGGATCGTAGGAATCAACAA
KISS1_F	GGCTTCTCTTGGTGTGTTCC
KISS1_R	TCATTCTGGCAGGAAGAGGC
COL2A1_F	TGGGTGTTCTATTTATTTATTGTCTTCCT
COL2A1_R	GCGTTGGACTCACACCAGTTAGT
RUNX2_F	GACGAGGCAAGAGTTTCACC
RUNX2_R	GGACCGTCCACTGTCACTTT

Data Analysis

Data analysis was completed using the SigmaPlot Software version 14.5. One-way or Two-way ANOVA analyses were performed, and differences were considered significant at ($P < 0.05$) using the Holm-Sidak test. Other depictions created using BioRender.com .

Results:

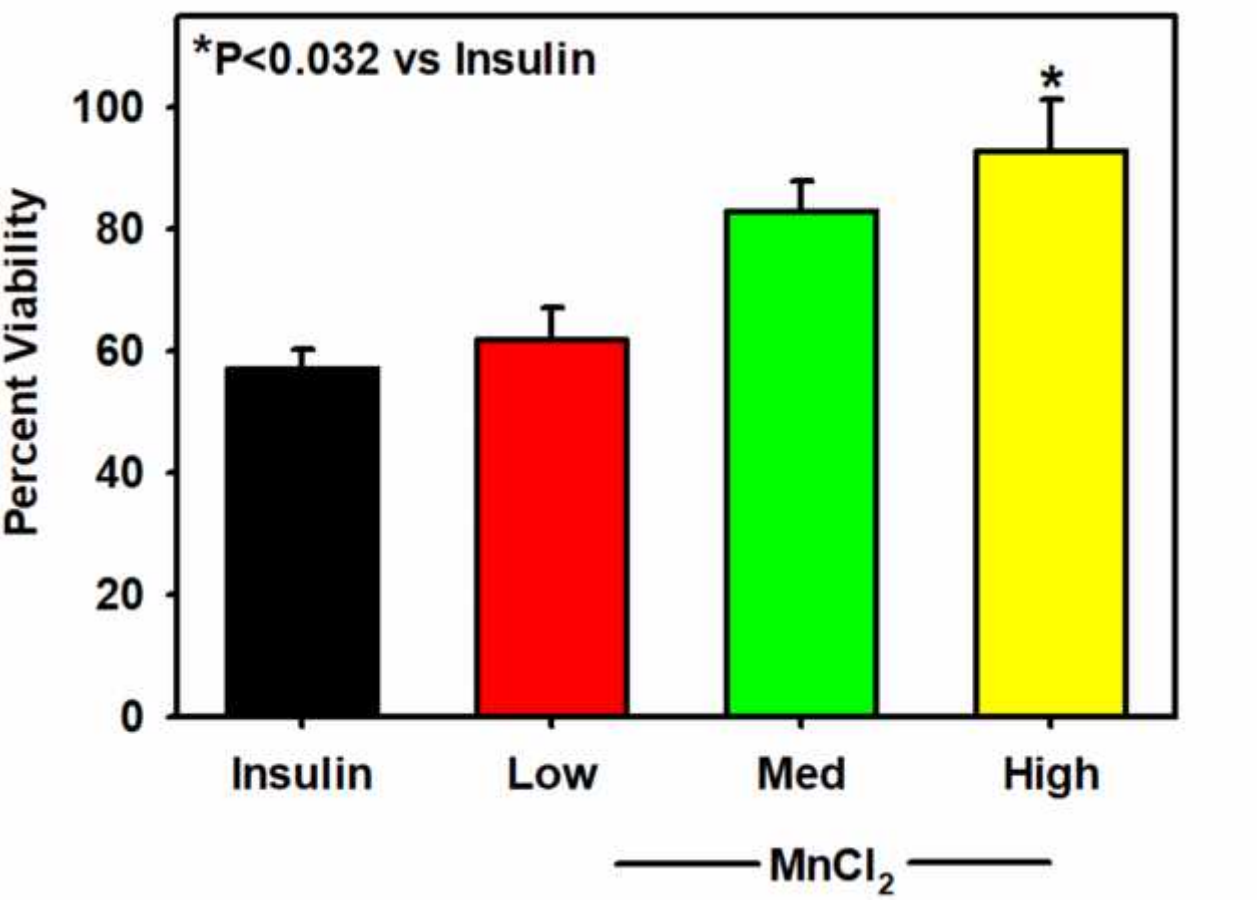

Figure 3: Quantification of Cell Proliferation in Trace Element Treated ATDC5 Cells
*$MnCl_2$ displayed a significant increase between insulin and high dose (*P<0.032, n=3). Increasing concentration of $MnCl_2$ demonstrated positive correlation with Percent Viability.*

$MnCl_2$ Affects Cellular Viability

Percent viability of the Low dose increased 0.03-fold when compared to Insulin and 0.38-fold of the medium dose when compared to insulin **(Figure 1).** No statistical difference was found between the low and medium doses when compared to insulin. However, high dose $MnCl_2$ was found to be 0.5-fold significant increase when compared to insulin (*P<0.032).

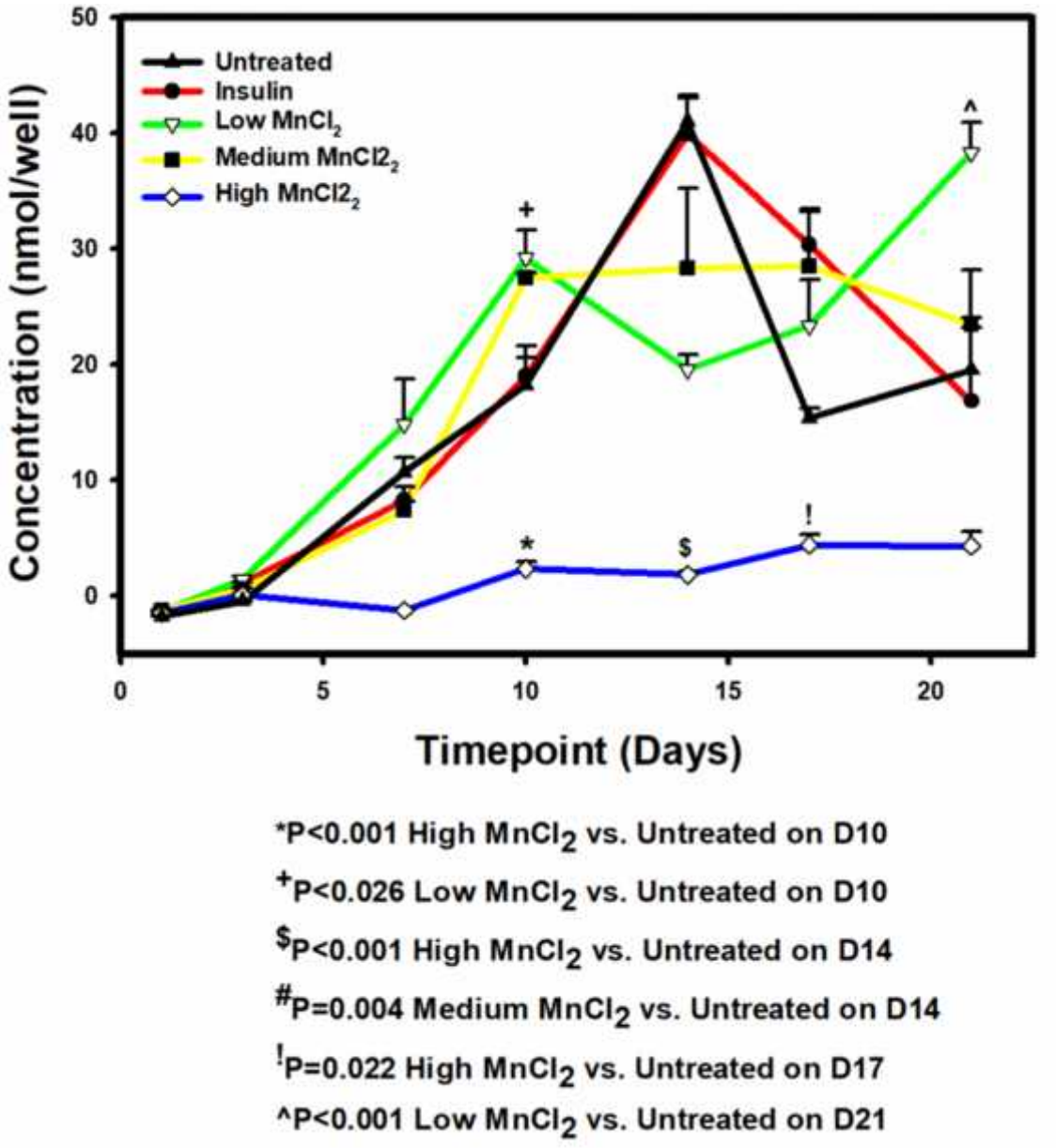

Figure 4: ALP Activity in Trace Element Treated ATDC5 Cells Over 21 Days
There is a statistically significant interaction between Time and Treatment. (P = <0.001, n=3). Refer to ***Tables 4 and 5*** *for the significant P-values.*

$MnCl_2$ Treatment Stimulates Alkaline Phosphatase Activity

Our data shows that all treatment groups, except high $MnCl_2$, show increased ALP activity between days 1 and 10 **(Figure 4, Tables 4, 5).** There were no statistically significant differences on days 1 to 7. A >1.5-fold significant increase was detected on day 10 when comparing low and medium $MnCl_2$ to untreated and insulin groups ($^{+}P<0.026$). When comparing day 10 low and medium $MnCl_2$ to high $MnCl_2$, there was a 14.5-fold increase ($P<0.001$). The high $MnCl_2$ treatment group significantly decreased ALP treatment at all time points when compared to untreated (*$P<0.001$ on days 10 and 14, $^{!}P=0.022$ on day 17). Low and medium $MnCl_2$ treatments are 2.1-fold and 1.4-fold less than both untreated and insulin-treated on day 14, respectively ($P<0.001$). However, on day 21, the low $MnCl_2$ treatment group had 2.0-fold significantly higher ALP levels then both untreated and insulin treatment groups (^$P<0.001$).

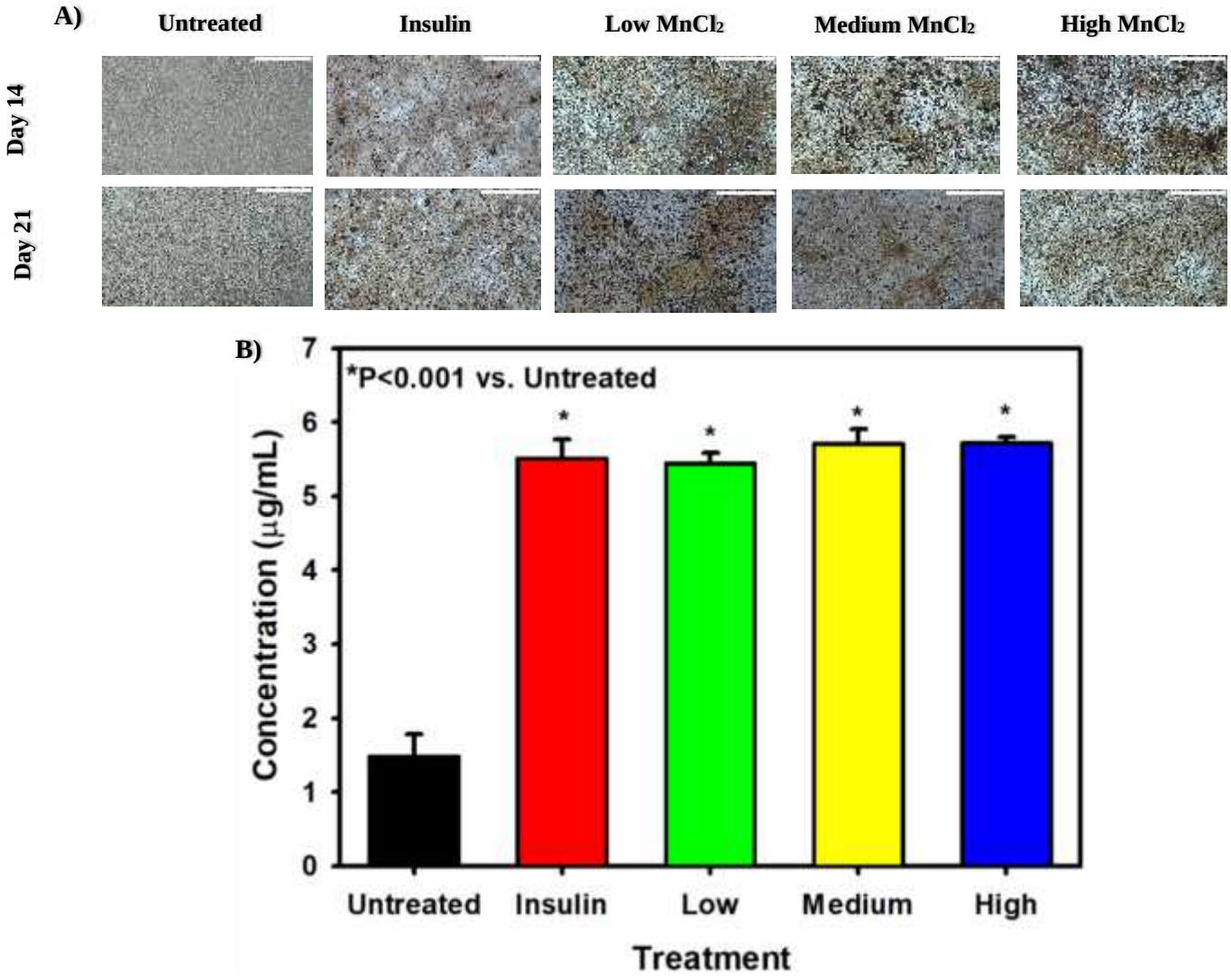

Figure 5: Calcium Deposition in ATDC5 Cells Post $MnCl_2$ Treatment

A) Qualitative Staining of ATDC5 Cells with Alizarin Red on D14 and D21 at 4x Magnification Scale bar measures 500 micrometers.

B) Quantitative Measures of D21 Alizarin Red Concentrations across all treatments show statistical significance when compared to untreated cells, ($P<0.001$, $n=3$).

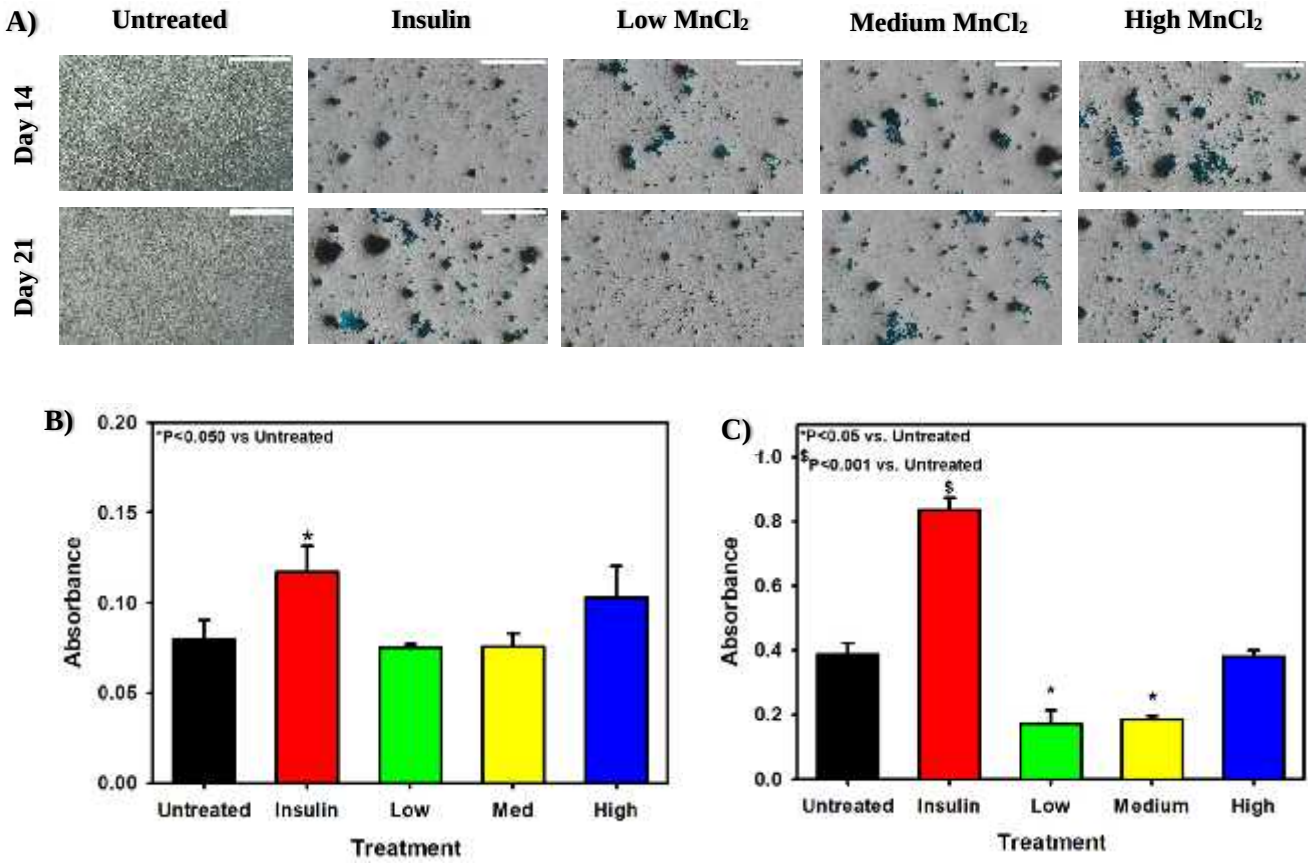

Figure 6: Proteoglycan Deposition in ATDC5 Cells Post $MnCl_2$ Treatment on Days 14 & 21

A) Qualitative Staining of ATDC5 Cells with Alcian Blue on D14 and D21 at 4x Magnification Scale bar measures 500 micrometers.

*B) Proteoglycan Deposition of Trace Elements Treated ATDC5 Cells on Day 14 There was a significant difference between the untreated and insulin treated groups (*P<0.05, n=3).*

*C) Proteoglycan Deposition of Trace Elements Treated ATDC5 Cells on Day 21 The treatment groups displayed varying concentrations of proteoglycan deposition with only the low and medium treatment significant when compared to untreated (*P<0.005, n=2)*

$MnCl_2$ Induces Calcification and Proteoglycan Deposition in ATDC5 Chondrocytes

Low, medium, and high doses clearly show larger amounts of chondrocyte condensation as visualized by increased red-brown pigment and the large clusters of condensate calcified nodules when compared to the untreated control **(Figure 5A)**. On day 21, calcification was quantified, where all treatment groups showed a 4.0-fold significant difference of calcium deposition when compared to untreated cells (*P<0.001, **Figure 5B)**. Qualitative analysis (**Figure 6A**) shows an increase in blue pigmentation when treating chondrocytes with insulin on both days 14 and 21. Untreated, low $MnCl_2$, medium $MnCl_2$ groups were found to be 1.4-fold and 0.25-fold significantly less than insulin-treatment on day 14 and day 21, respectively. On day 21, low and med $MnCl_2$ were 3.0-fold significantly less than the untreated group as well (*P<0.05, **Figure 6C).**

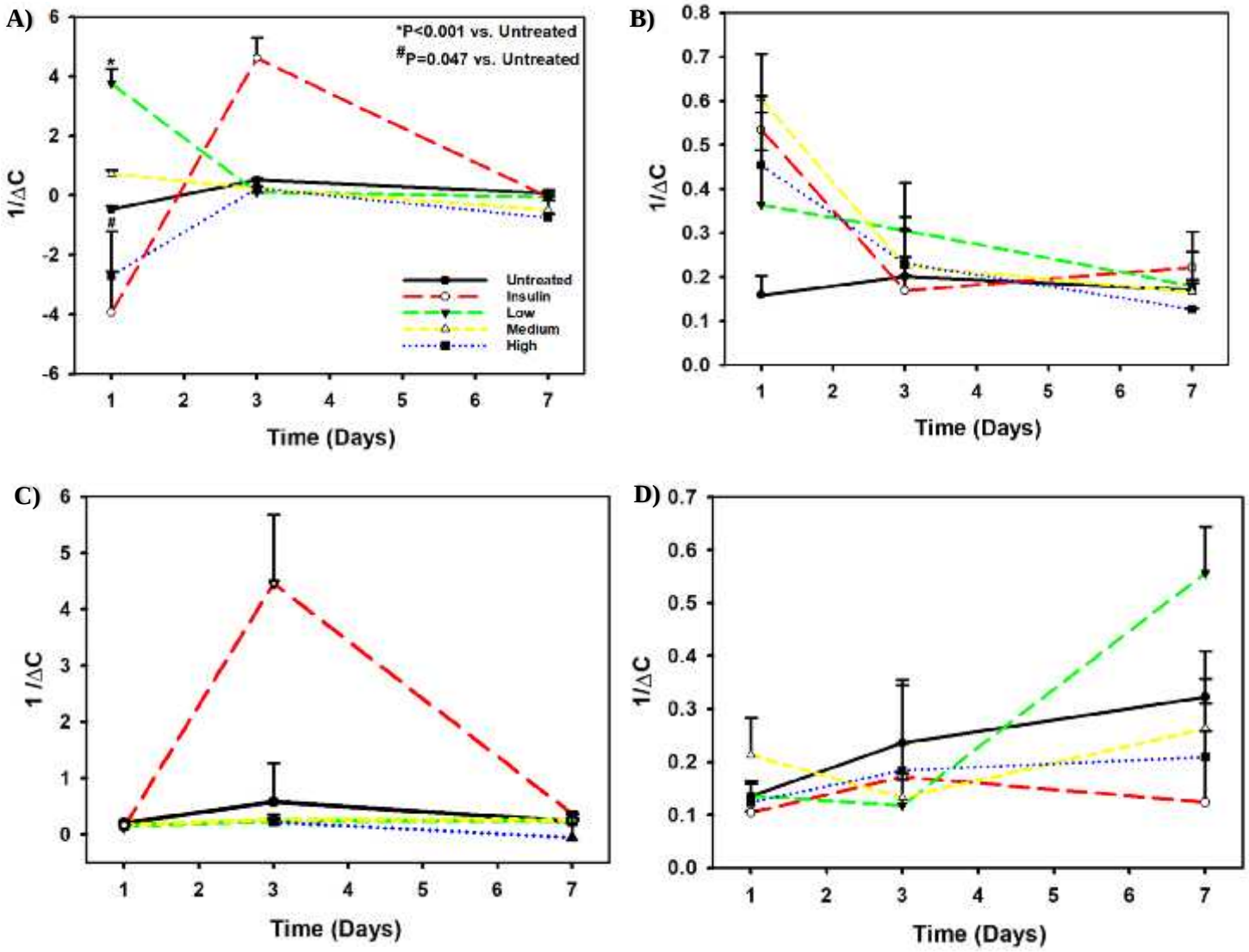

Figure 7: Quantification of Gene Expression Post $MnCl_2$-Treatment Overtime

*A) Col2a1 Expression in low and high $MnCl_2$ treated cells shows greatest activity on Day 1 in comparison to Untreated cells (*P<0.001, #P=0.047, n=2).*

B) RUNX2 Expression is increased with $MnCl_2$ and insulin at Day 1, which decreases overtime to Day 7 (n=2).

C) RHEB Expression shows minimal activity in $MnCl_2$ treated cells. Insulin is increased compared to treatment groups (n=3).

D) KISS1 Expression in medium and high $MnCl_2$ show decreased KISS1activity compared to untreated cells. Low $MnCl_2$ shows heighted KISS1 expression at Day 7 (n=3).

Characterization of Gene Expression in $MnCl_2$ Treated ATDC5 Cells

When investigating Col2a1 expression on day 1, low $MnCl_2$ was found to have increased gene expression when compared to untreated, insulin and high $MnCl_2$ treatment groups ($P<0.001$). Day 1 medium $MnCl_2$ also displayed a similar trend against insulin and high $MnCl_2$ ($P<0.001$, $P=0.004$). On day 3, Col2a1 expression was most seen upregulated in the insulin treatment group when compared to the other treatment groups ($P<0.001$, **Figure 7A)**. Insulin and $MnCl_2$ treatment groups have increased RUNX2 activity on Day 1, but declined by Day 7 (**Figure 7B**). $MnCl_2$ -treatments on Days 1, 3, and 7 show little to no expression of RHEB in ATDC5 cells (**Figure 7C**). On day 3, insulin treatment shows increased RHEB expression. KISS1 activity increased in untreated samples between days 1-7. On day 1, a significant increase in KISS1 expression was found when comparing medium $MnCl_2$ and all other treatment groups. By day 7, the low $MnCl_2$ group showed 0.27-fold increase in the KISS1 expression when compared to all other treatment groups (**Figure 7D**).

Discussion & Conclusion:

In this study, it was hypothesized that manganese chloride would have a positive effect on chondrocyte viability, alkaline phosphatase (ALP) activity, calcium deposition, and proteoglycan deposition. $MnCl_2$ was found to decrease cellular viability at all concentrations (0.3µM-30µM) when compared to our untreated control. Our data is similar to Doyle et al who found that 10µM of manganese chloride inhibited cell viability and differentiation by 50% in micromass cultures of mouse embryonic limb bud cells using a neutral red biouptake assay (19). Similarly, Lüthen et al, who studied the cellular behavior of manganese ions on human osteoblasts *in vitro*, found that in a manganese concentration-dependent manner human osteoblast cellular morphology was altered and growth inhibited (20). A neurotoxicity study conducted by Cardova et al found that prolonged manganese exposure increased ROS and caspase activity, initiating apoptotic and necrotic cell death of *in vivo* rat models (21). Thus, the increased oxidative stress could explain the decrease in cellular viability of our ATDC5 cells.

Interestingly, we found that despite of reductions in cell viability or proliferation the presence of $MnCl_2$ at low or medium levels had positive effects on calcium deposition. Previous data supports are finding that lower concentrations of $MnCl_2$ (0.125mg/kg) aids in fracture healing after day 10 by significantly increasing precent mineralization of tissue ($P<0.05$) as in Hreha et al (22). This confirms that $MnCl_2$ treatments can induce the secretion of proper proteins for endochondral ossification, including calcium. According to Litchfield et al, manganese concentrations of 50µM or higher inhibit mineralization of primary chondrocytes from broiler-strain chickens, reducing levels of proteoglycan, cell proteins, and collagen synthesis (23). Regarding proteoglycan deposition, we found the $MnCl_2$ impaired its deposition at as little as

0.3µM. Similarly, Doyle's observed fewer proteoglycan-producing nodules in manganese-exposed cultures of mouse embryonic limb bud cells on day 21 (19). Doyle noted that the number of proteoglycan-producing nodules reduced 50% when comparing 20µM MnCl2 to the untreated control (19).

Overall, we found that $MnCl_2$ can modulate gene expression of Col2a1, RUNX2, RHEB, and KISS1. Cells treated with $MnCl_2$ peaked in Col2a1 expression, a marker of MSC condensation and major component of the ECM on day 1. Through the lens of OA, Kumar et al investigated inflammation-induced cartilage protection with manganese dioxide (MnO_2) nanoparticles (24). Like our findings, Kumar found that the expression of catabolic genes, such as Col2a1, were upregulated with the addition of MnO_2 nanoparticles (24). Prasadh, who studied manganese containing alloy extracts cultured with osteoblastic MC3T3-E1 cells, saw an increase of RUNX2 and ALP expression (25). The upregulation of RUNX2 and ALP reflect hypertrophic chondrocytes differentiation, mineralization, and endochondral ossification, confirming our ALP results. Sato, who studied Mn^{2+} activation on recombinant RHEB proteins that were purified after expression in *E. Coli,* RHEB does not activate the catalytic activity of mTOR, but Mn^{2+}can directly activate mTOR's subunit, mTORC1, even without RHEB present (26). In terms of chondrogenesis, the activation of mTORC1 is crucial for embryonic skeletal growth and matrix production (27). As confirmed by Sato, our data displays a downregulation of RHEB expression throughout the 7 days of treatment. Interestingly, Sato also found that Insulin activates RHEB through AKT-dependent phosphorylation of TSC2, which also activates mTORC1 (26). Sato's data confirms the increased gene expression of RHEB with our positive control, insulin (26). According to Srivastava, who investigated KISS1 stimulation with manganese in prepubertal

female rats, concluded that manganese increased AKT, RHEB, TSC2, and KISS1, which all serve as activators of the mTOR pathway (18).

In conclusion, $MnCl_2$ reduced cellular viability and proteoglycan deposition, while increasing ALP activity and calcium deposition. Col2a1expression of $MnCl_2$ treated cells was statistically significant at the beginning of chondrogenesis, but reduces RUNX2 activity up to day 7. Further analysis of transcription factors, such as SOX9 and BMPs, can also be reviewed on the gene and protein level to understand where cellular viability and proteoglycan levels begin to dwindle. For this, earlier timepoints between 8 hours and 72 hours can be tested, as much of our data points to either elevated or decreased activity on day 3. Additionally, our results demonstrated downregulation of RHEB expression, while KISS1 displayed slowly increasing expression over 7 days. Further experiments investigating manganese as an insulin-mimetic can be conducted to understand the element's role in pathway modulation. Previous studies have explored insulin or IGF treatments improving neurodegenerative Huntington Disease via the PI3K/AKT/mTOR pathway, and have also revealed that manganese is able to activate many of the same metabolic kinases, while increasing peripheral and neuronal insulin and IGF-1 levels in rodent models (28). Also, other studies have confirmed *in vitro* manganese exposure activates extracellular signal-related protein kinase-1/2 (ERK1/2) and AKT phosphorylation (21). Considering this, different activators of the PI3K/AKT/mTOR pathway can be explored to better understand manganese's role in chondrogenesis.

Supplemental Data:

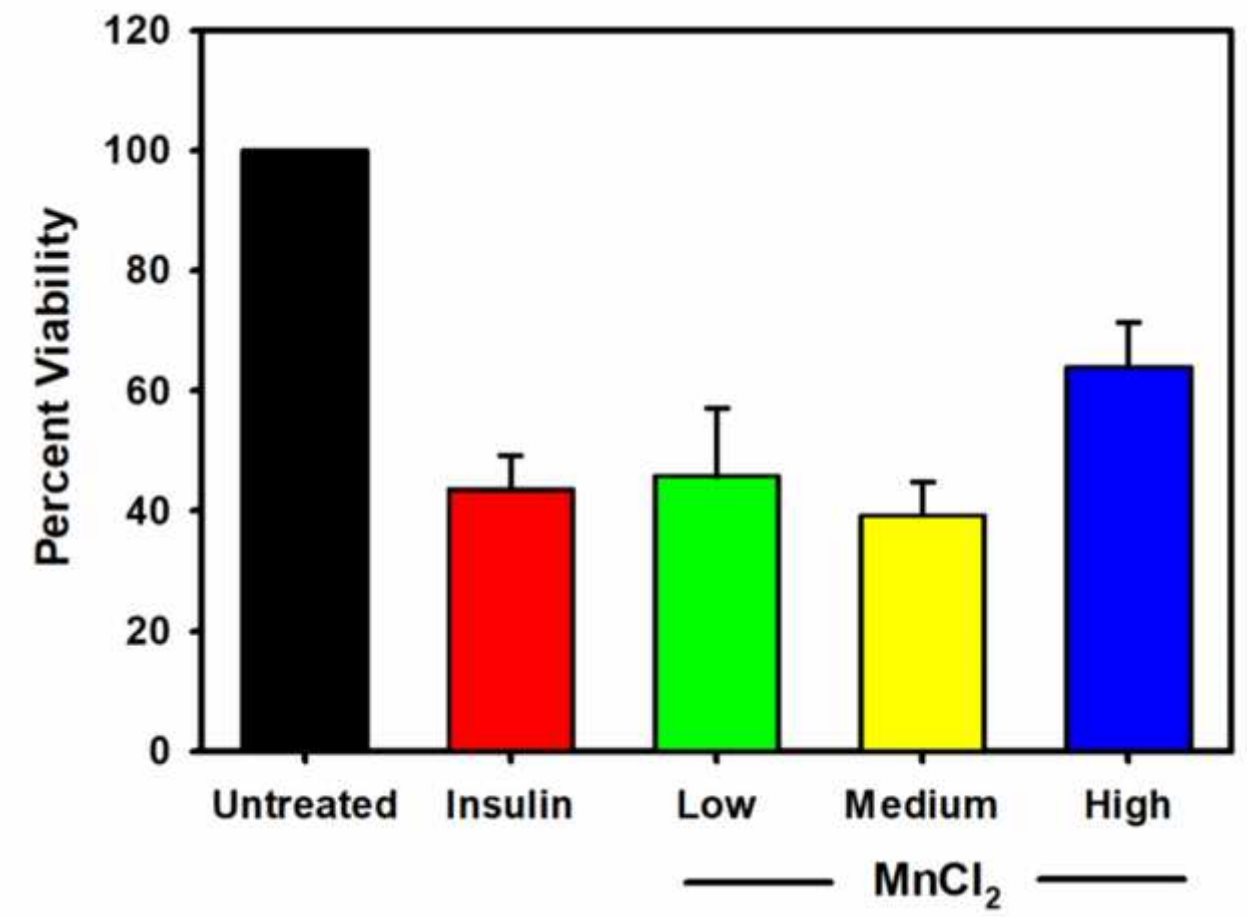

Figure A: Quantification of Cell Proliferation in Trace Element Treated MC3T3-E1 Cells
Manganese chloride treatments showed no statistical significance on the murine osteoblast cell line, MC3T3-E1 (n=6).

Table 4: Comparison of Significant Treatments of ALP Activity Per Day

Day 10		Day 14		Day 17		Day 21	
Comparison	**P-Value**	**Comparison**	**P-Value**	**Comparison**	**P-Value**	**Comparison**	**P-Value**
Low vs. High	<0.001	Untreated vs. High	<0.001	Positive vs. High	<0.001	Low vs. High	<0.001
Medium vs. High	<0.001	Positive vs. High	<0.001	Medium vs. High	<0.001	Low vs. Medium	<0.001
Positive vs. High	<0.001	Medium vs. High	<0.001	Low vs. High	<0.001	Low vs. Positive	<0.001
Untreated vs. High	<0.001	Untreated vs. Low	<0.001	Positive vs. Untreated	<0.001	Low vs. Untreated	<0.001
Low vs. Untreated	0.026	Positive vs. Low	<0.001	Medium vs. Untreated	0.004	Untreated vs. High	<0.001
Low vs. Positive	0.04	Low vs. High	<0.001	Untreated vs. High	0.022	Positive vs. High	0.006
		Untreated vs. Medium	0.004			Medium vs. High	0.027
		Positive vs. Medium	0.008				
		Medium vs. Low	0.044				

Table 5: Comparison of Significant Timepoints of ALP Activity Per Treatment

Untreated		Insulin		Low		Medium	
Day	**P-Value**	**Day**	**P-Value**	**Day**	**P-Value**	**Day**	**P-Value**
D7 vs. D1	0.012	D10 vs. D1	<0.001	D7 vs. D1	<0.001	D10 vs. D1	<0.001
D7 vs. D3	0.031	D10 vs. D3	<0.001	D7 vs. D3	0.005	D10 vs. D21	0.008
D10 vs. D1	<0.001	D10 vs. D7	0.035	D10 vs. D1	<0.001	D10 vs. D3	<0.001
D10 vs. D3	<0.001	D14 vs. D1	<0.001	D10 vs. D3	<0.001	D10 vs. D7	<0.001
D14 vs. D1	<0.001	D14 vs. D10	<0.001	D10 vs. D7	0.002	D14 vs. D1	<0.001
D14 vs. D10	<0.001	D14 vs. D21	<0.001	D14 vs. D1	<0.001	D14 vs. D21	0.004
D14 vs. D17	<0.001	D14 vs. D3	<0.001	D14 vs. D3	<0.001	D14 vs. D3	<0.001
D14 vs. D21	<0.001	D14 vs. D7	<0.001	D17 vs. D1	<0.001	D14 vs. D7	<0.001
D14 vs. D3	<0.001	D17 vs. D1	<0.001	D17 vs. D3	<0.001	D17 vs. D1	<0.001
D14 vs. D7	<0.001	D17 vs. D10	0.027	D21 vs. D1	<0.001	D17 vs. D21	0.004
D17 vs. D1	<0.001	D17 vs. D21	0.005	D21 vs. D14	<0.001	D17 vs. D3	<0.001
D17 vs. D3	<0.001	D17 vs. D3	<0.001	D21 vs. D17	0.001	D17 vs. D7	<0.001
D21 vs. D1	<0.001	D17 vs. D7	<0.001	D21 vs. D3	<0.001	D21 vs. D1	<0.001
D21 vs. D3	<0.001	D21 vs. D1	<0.001	D21 vs. D7	<0.001	D21 vs. D3	0.003
		D21 vs. D3	<0.001				

Table 6: Statistically Significant Treatments Within Timepoints

COL2a1			
Day 1		**Day 3**	
Comparison	**P-Value**	**Comparison**	**P-Value**
Low vs. Insulin	<0.001	Insulin vs. Low	<0.001
Low vs. High	<0.001	Insulin vs. Medium	<0.001
Medium vs. Insulin	<0.001	Insulin vs. High	<0.001
Low vs. Untreated	<0.001	Insulin vs. Untreated	0.001
Untreated vs. Insulin	0.005		
Medium vs. High	0.004		
Low vs. Medium	0.009		
Untreated vs. High	0.047		

References:

(1) "Manganese." *Mount Sinai Health System*, https://www.mountsinai.org/health-library/supplement/manganese

(2) Jianmei Li, Cuijun Deng, Wanyuan Liang, Fei Kang, Yun Bai, Bing Ma, Chengtie Wu, Shiwu Dong. Mn-containing bioceramics inhibit osteoclastogenesis and promote osteoporotic bone regeneration via scavenging ROS. Bioactive Materials. Volume 6, Issue 11. 2021. Pages 3839-3850. ISSN 2452-199X. https://doi.org/10.1016/j.bioactmat.2021.03.039. https://www.sciencedirect.com/science/article/pii/S2452199X2100150X

(3) Harvard School of Public Health. (2022, September 15). Manganese. The Nutrition Source. Retrieved November 28, 2022, from https://www.hsph.harvard.edu/nutritionsource/manganese/

(4) S. Ashraf, B.J. Kim, S. Park, H. Park, S.-H. Lee, RHEB gene therapy maintains the chondrogenic characteristics and protects cartilage tissue from degenerative damage during experimental murine osteoarthritis, Osteoarthritis and Cartilage, Volume 27, Issue 10, 2019, Pages 1508-1517, ISSN 1063-4584, https://doi.org/10.1016/j.joca.2019.05.024.

(5) Chen Hui, Tan Xiao-Ning, Hu Shi, Liu Ren-Qin, Peng Li-Hong, Li Yong-Min, Wu Ping. (2021). Molecular Mechanisms of Chondrocyte Proliferation and Differentiation. *Frontiers in Cell and Developmental Biology*, Vol. 9.

(6) Akkiraju, H., & Nohe, A. (2015). Role of Chondrocytes in Cartilage Formation, Progression of Osteoarthritis and Cartilage Regeneration. Journal of Developmental Biology, 3(4), 177–192. MDPI AG. Retrieved from http://dx.doi.org/10.3390/jdb3040177

(7) Goldring MB. Chondrogenesis, chondrocyte differentiation, and articular cartilage metabolism in health and osteoarthritis. Therapeutic Advances in Musculoskeletal Disease. August 2012:269-285. Doi:10.1177/1759720X12448454

(8) Sato T, Umetsu A, Tamanoi F. Characterization of the Rheb-mTOR signaling pathway in mammalian cells: constitutive active mutants of Rheb and mTOR. Methods Enzymol. 2008;438:307-20. Doi: 10.1016/S0076-6879(07)38021-X. PMID: 18413257; PMCID: PMC2693245.

(9) Wang, C. Y., Xia, W. H., Wang, L., & Wang, Z. Y. (2021). Manganese deficiency induces avian tibial dyschondroplasia by inhibiting chondrocyte proliferation and differentiation. *Research in veterinary science*, *140*, 164–170. https://doi.org/10.1016/j.rvsc.2021.08.018

(10) Wang, J., Wang, Z.Y., Wang, Z.J. et al. Effects of manganese deficiency on chondrocyte development in tibia growth plate of Arbor Acres chicks. J Bone Miner Metab 33, 23–29 (2015). https://doi.org/10.1007/s00774-014-0563-0

(11) Centers for Disease Control and Prevention. (2020, July 27). *Osteoarthritis (OA)*. Centers for Disease Control and Prevention. Retrieved September 8, 2022, from https://www.cdc.gov/arthritis/basics/osteoarthritis.htm#:~:text=Swelling-,How%20many%20people%20have%20OA%3F,over%2032.5%20million%20US%20adults.

(12) Ashraf, S., Ahn, J., Cha, B.-H., Kim, J.-S., Han, I., Park, H., and Lee, S.-H. (2017) RHEB: a potential regulator of chondrocyte phenotype for cartilage tissue regeneration. *J Tissue Eng Regen Med*, 11: 2503– 2515. Doi: 10.1002/term.2148

(13) Mayo Foundation for Medical Education and Research. (2021, June 16). *Osteoarthritis*. Mayo Clinic. Retrieved September 8, 2022, from https://www.mayoclinic.org/diseases-conditions/osteoarthritis/diagnosis-treatment/drc-20351930

(14) Madry, H. and Cucchiarini, M. (2013), Advances and challenges in gene-based approaches for osteoarthritis. J Gene Med, 15: 343-355. https://doi.org/10.1002/jgm.2741

(15) Li G, Cheng T, Yu X. The Impact of Trace Elements on Osteoarthritis. Front Med (Lausanne). 2021 Dec 23;8:771297. Doi: 10.3389/fmed.2021.771297. PMID: 35004740; PMCID: PMC8732765.

(16) Zhang Y, Vasheghani F, Li Y, et al. Cartilage-specific deletion of mTOR upregulates autophagy and protects mice from osteoarthritis. Annals of the Rheumatic Diseases 2015;74:1432-1440.

(17) Raffaele Nicastro, Hélène Gaillard, Laura Zarzuela, Marie-Pierre Péli-Gulli, Elisabet Fernández-García, Mercedes Tomé, Néstor García-Rodríguez, Raúl V Durán, Claudio De Virgilio, Ralf Erik Wellinger (2022) Manganese is a physiologically relevant TORC1 activator in yeast and mammals eLife 11:e80497. https://doi.org/10.7554/eLife.80497

(18) Vinod K. Srivastava, Jill K. Hiney, William L. Dees, Manganese-Stimulated Kisspeptin Is Mediated by the IGF-1/Akt/Mammalian Target of Rapamycin Pathway in the Prepubertal Female Rat, *Endocrinology*, Volume 157, Issue 8, 1 August 2016, Pages 3233–3241, https://doi.org/10.1210/en.2016-1090

(19) D Doyle, C.M Kapron, Inhibition of cell differentiation by manganese chloride in micromass cultures of mouse embryonic limb bud cells, Toxicology in Vitro, Volume 16,

Issue 2, 2002, Pages 101-106, ISSN 0887-2333, https://doi.org/10.1016/S0887-2333(01)00109-6.

(20) Lüthen, F., Bulnheim, U., Müller, P. D., Rychly, J., Jesswein, H., & Nebe, J. G. (2007). Influence of manganese ions on cellular behavior of human osteoblasts in vitro. *Biomolecular engineering*, *24*(5), 531–536. https://doi.org/10.1016/j.bioeng.2007.08.003

(21) Cordova FM, Aguiar AS Jr, Peres TV, Lopes MW, Gonçalves FM, et al. (2012) In Vivo Manganese Exposure Modulates Erk, Akt and Darpp-32 in the Striatum of Developing Rats, and Impairs Their Motor Function. PLOS ONE 7(3): e33057. https://doi.org/10.1371/journal.pone.0033057

(22) Hreha, J., Wey, A., Cunningham, C., Krell, E.S., Brietbart, E.A., Paglia, D.N., Montemurro, N.J., Nguyen, D.A., Lee, Y.-J., Komlos, D., Lim, E., Benevenia, J., O'Connor, J.P. and Lin, S.S. (2015), Local manganese chloride treatment accelerates fracture healing in a rat model. J. Orthop. Res., 33: 122-130. https://doi.org/10.1002/jor.22733

(23) Litchfield, T., Ishikawa, Y., Wu, L. *et al.* Effect of Metal Ions on Calcifying Growth Plate Cartilage Chondrocytes. *Calcif Tissue Int* **62**, 341–349 (1998). https://doi.org/10.1007/s002239900442

(24) Kumar, S., Adjei, I. M., Brown, S. B., Liseth, O., & Sharma, B. (2019). Manganese dioxide nanoparticles protect cartilage from inflammation-induced oxidative stress. *Biomaterials*, *224*, 119467. https://doi.org/10.1016/j.biomaterials.2019.119467

(25) Prasadh, S., Gupta, M. & Wong, R. In vitro cytotoxicity and osteogenic potential of quaternary Mg-2Zn-1Ca/X-Mn alloys for craniofacial reconstruction. *Sci Rep* **12**, 8259

(2022). https://doi.org/10.1038/s41598-022-12490-0

https://www.frontiersin.org/articles/10.3389/fcell.2021.664168

(26) Sato, T., Nakashima, A., Guo, L., & Tamanoi, F. (2009). Specific activation of mTORC1 by Rheb G-protein in vitro involves enhanced recruitment of its substrate protein. *The Journal of biological chemistry*, *284*(19), 12783–12791. https://doi.org/10.1074/jbc.M809207200

(27) Chen, J., & Long, F. (2014). mTORC1 signaling controls mammalian skeletal growth through stimulation of protein synthesis. *Development (Cambridge, England)*, *141*(14), 2848–2854. https://doi.org/10.1242/dev.108811

(28) Bryan, M.R., Bowman, A.B. (2017). Manganese and the Insulin-IGF Signaling Network in Huntington's Disease and Other Neurodegenerative Disorders. In: Aschner, M., Costa, L. (eds) Neurotoxicity of Metals. Advances in Neurobiology, vol 18. Springer, Cham. https://doi.org/10.1007/978-3-319-60189-2_6